Available online at www.sciencedirect.com
ScienceDirect
Corrosion Science 50 (2008) 1149–1155
CORROSION SCIENCE
www.elsevier.com/locate/corsci

Determination of the sensitized zone extension in welded AISI 304 stainless steel using non-destructive electrochemical techniques

Pedro de Lima-Neto [a,*], Jesualdo P. Farias [b], Luis Flávio G. Herculano [a,b], Hélio C. de Miranda [b], Walney S. Araújo [b], Jean-Baptiste Jorcin [c], Nadine Pébère [c]

[a] Departamento de Química Analítica e Físico-Química, Universidade Federal do Ceará, Campus do Pici, Bloco 940, 60455-970, Fortaleza, CE, Brazil
[b] Departamento de Engenharia Metalúrgica e Materiais, Universidade Federal do Ceará, Campus do Pici, Bloco 714, 60455-970, Fortaleza, CE, Brazil
[c] CIRIMAT – UMR CNRS 5085, ENSIACET, 118 route de Narbonne, 31077 Toulouse cedex 04, France

Received 10 July 2007; accepted 28 July 2007
Available online 18 January 2008

Abstract

Extension of sensitized zone (SZ) in welded AISI 304 stainless steel was determined by two non-destructive electrochemical tests: double loop electrochemical potentiokinetic reactivation technique (DLEPR) and local electrochemical impedance spectroscopy (LEIS). Welding was carried out using the shielded metal arc with two selected welding energies: the first one ($0.7\,kJ\,mm^{-1}$) does not promote the sensitization of the 304 steel and it constitutes the reference sample and the second one ($2.2\,kJ\,mm^{-1}$) which leads to the precipitation of chromium carbides in the grain boundaries after the welding process. The non-destructive DLEPR and LEIS tests allowed the length of the SZ to be determined and a good agreement between the two techniques and the microstructure of the two welded samples was shown. The presence of an inductive loop on the local impedance diagrams seems to reflect a galvanic coupling between the weld string (anode) and the welded stainless steel plates (cathode) which will be very prejudicial to a good corrosion resistance of the welded system. The results showed that the two electrochemical tests could be applied in practical cases in industrial field.

Keywords: A. Stainless steel; B. EIS; B. SEM; C. Welding; C. Intergranular corrosion

1. Introduction

It is widely known that welded austenitic stainless steels can present a sensitized zone (SZ) in the heat affected zone (HAZ). This is a well-known phenomenon and consists of carbide precipitation at grain boundaries and chromium depletion in adjacent regions, making the material susceptible to intergranular corrosion. The intensity of this phenomenon is affected by, among other factors, the amount of carbon in the base material and in the welded material, the welding process, the welding energy, the exposure time of the material to the temperature in that segregation phenomena take place and the carbide maker elements [1].

Usually, the sensitized region is determined by methodologies mentioned in ASTM A262 Standard Practice. However, this standard does not quantify the sensitization degree, the tests are of difficult preparation, exclusive for use in laboratory and they are destructive. For an industrial practice point of view, it is necessary to develop non-destructive methods and tests for the assessment of sensitized zone in a welded stainless steel on its site of operation.

Double loop electrochemical potentiokinetic reactivation test (DLEPR) is a powerful tool used recently in our laboratory to evaluate the sensitization to quantify the degree of sensitization of five austenitic stainless steels (304, 304L, 316L, 321 and 347) heat treated in the range of 400 °C–600 °C for until 100 hours [2,3], to study the loss of the corrosion resistance of the UNS S31803 duplex stainless steel aged at low temperatures (350–550 °C) [4] and finally, to assess the effect of the low-temperature aging in the corrosion

* Corresponding author. Tel.: +55 85 33669956; fax: +55 85 33669982.
E-mail address: pln@ufc.br (P. de Lima-Neto).

0010-938X/$ - see front matter © 2007 Elsevier Ltd. All rights reserved.
doi:10.1016/j.corsci.2007.07.014

resistance of AISI 444 stainless steel [5]. The advantages of this technique are: it is quick, non-destructive, could be used for *in situ* measurements and the results are independent of the surface finishing.

Local electrochemical impedance spectroscopy (LEIS) is also another non-destructive electrochemical technique that has been used in recent years to study localized corrosion on bare metal surface and on coated alloys [6,7]. Additionally, sensitization is a localized phenomenon which turns interesting to apply the LEIS technique to localize the sensitized region in a welding stainless steel.

Thus, the aim of the present work is to evaluate the potentiality of the DLEPR and LEIS techniques to determine the extension of the sensitized area in a welded AISI 304 stainless steel. The study was carried out using two selected welding energies: 0.7 kJ mm^{-1}, which does not promote the sensitization of the 304 steel and used as reference, and 2.2 kJ mm^{-1} to obtain the precipitation of chromium carbides in the grain boundaries after the welding process.

2. Experimental

2.1. Material and welding process

AISI 304 sheet, obtained from hot lamination process, was supplied by ACESITA (Brazil). The chemical composition was given by the manufacturer and is presented in Table 1. The composition is in agreement with the standard limits for the AISI 304 stainless steel. The steels were welded using shielded metal arc welding (SMAW) technique with the ARCHES AWS E – 308L – 16 electrode having 3.25 mm diameter. The welding parameters are presented in Table 2.

2.2. Metallographic etchings

Metallographic etching according to ASTM A-262 was performed. Micrographs were acquired using a Philips XL-30 scanning electron microscope (SEM). The obtained microstructures were classified into three types: "step" structure with no ditches at grain boundaries; "dual" structure, with some ditches at grain boundaries; and "ditch" structure, with one or more grains completely surrounded by ditches.

Table 1
Chemical composition of AISI 304 (% wt)

Element	C	Mn	Si	P	Cr	Ni	Mo
wt%	0.02	1.39	0.46	0.03	16.82	10.06	2.03
Element	V	Nb	Sn	Ti	N	W	Co
wt%	0.04	0.02	0.01	0.01	0.03	0.03	0.05

Table 2
Welding parameters

Current/A	Voltage/V	Travel speed/ mm min^{-1}	Welding energy/kJ mm^{-1}
92	24	200	0.7
132	28	100	2.2

SEM micrographs showing the microstructures, classified according ASTM A-262, can be found elsewhere [3].

2.3. DLEPR tests

The electrochemical cell was positioned on the HAZ of welded steel to analyse the extension of the sensitized region. Fig. 1 shows a draw of the system used for the DLEPR measurements and an O ring was used to maintain the solution in the cell exposing an area of 1 mm^2. Fig. 2a shows a schema of the different positions of the plate where the DLEPR measurements were performed.

Prior to each experiment, the welded AISI 304 steel surface was polished with 400 grit emery paper, degreased with ethanol and cleaned in water. The working solution was 0.5 M H_2SO_4 + 0.01 M KSCN. The DLEPR tests were conducted using a Pt foil as the auxiliary electrode and a saturated calomel electrode (SCE) as the reference one. The experiments were started after nearly steady-state open circuit potential (E_{oc}) had been reached (about 10 min) followed by the potential sweep in the anodic direction at 1 mV s^{-1} until the potential of 0.3 V/SCE was reached, then the scan was reversed until the E_{oc}. A potentiostat/galvanostat AUTOLAB PGSTAT 30, linked with a PC microcomputer and controlled by the GPES software, was used for acquisition of the electrochemical data.

2.4. LEIS measurements

LEIS technique was used to correlate the local electrochemical behaviour with the modification of the microstructure in

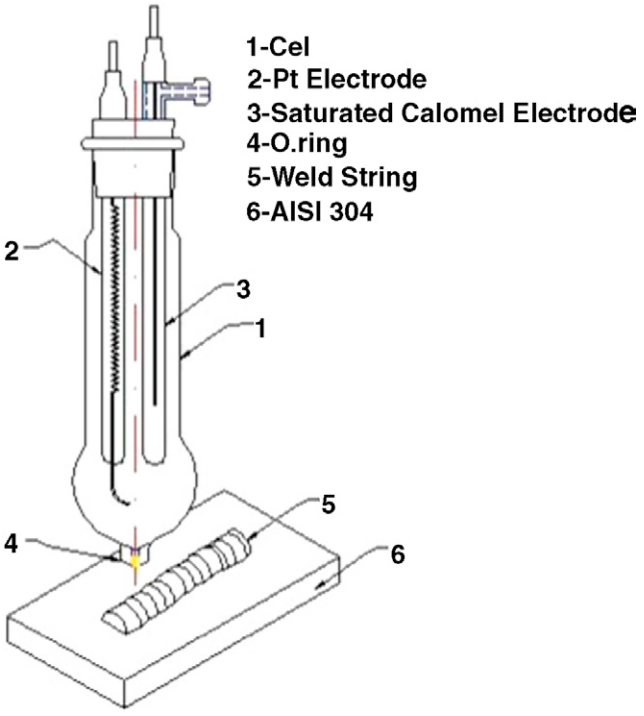

Fig. 1. Draw of the electrochemical cell used to evaluate the extension of the sensitized region in welded AISI 304 SS (DLEPR tests).

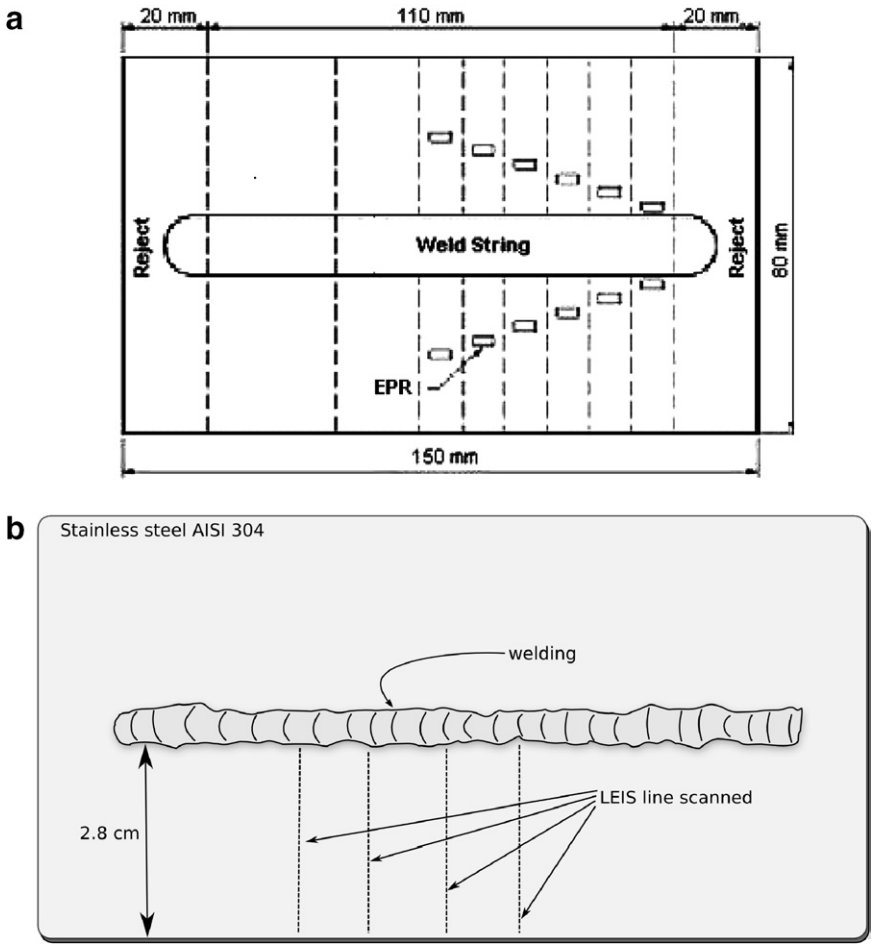

Fig. 2. Schematic representations of the welded plate. For the two electrochemical techniques, the different positions where the measurements were carried out are indicated on the scheme.

the HAZ of the studied welded material. LEIS measurements were carried out with a Solartron 1275 system. This method used a five-electrode configuration and details can be found elsewhere [6,7]. As in such a configuration the local measured current depends on the conductivity of the electrolyte. Thus, the experiments were carried out in 0.001 M Na_2SO_4 in order to improve the resolution of the method. The local impedance diagrams were obtained each 0.5 mm perpendicularly to the weld string (Fig. 2b) and were recorded over a frequency range of 10 kHz to around 100 MHz. With the used experimental set-up, only the normal component of the current was measured and the spatial resolution was estimated to be about 1 mm^2 for each measurement.

3. Results and discussion

3.1. Microstructure characterization

Fig. 3 shows a SEM image of the 304 SS surface, welded with 0.7 $kJ\,mm^{-2}$, and obtained at 4 mm from the weld string. It can be observed the absence of ditches on the grain boundaries. The observed microstructure was representative of that observed at different places in the HAZ of the welded 304 SS. This surface morphology, according to ASTM 262-A, is classified as step and associated to a non-sensitized stainless steel.

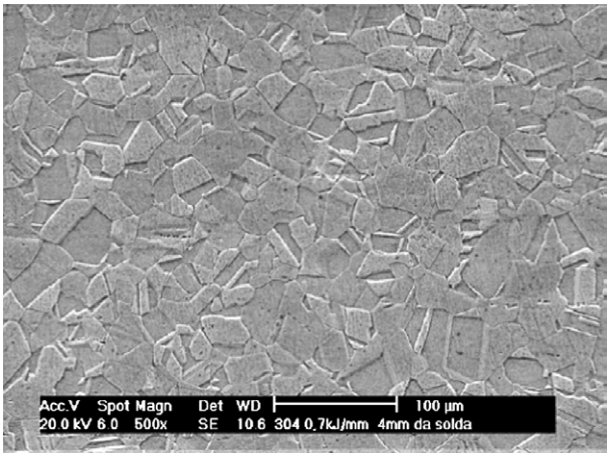

Fig. 3. SEM images showing a typical micrograph of the 304 SS welding with 0.7 $kJ\,mm^{-1}$. The micrograph was observed at 4 mm from the weld string.

The modification of the microstructure of the 304 SS, welded with 2.2 $kJ\,mm^{-2}$, with the distance from the weld string is shown in Fig. 4. The microstructure at 2 mm from

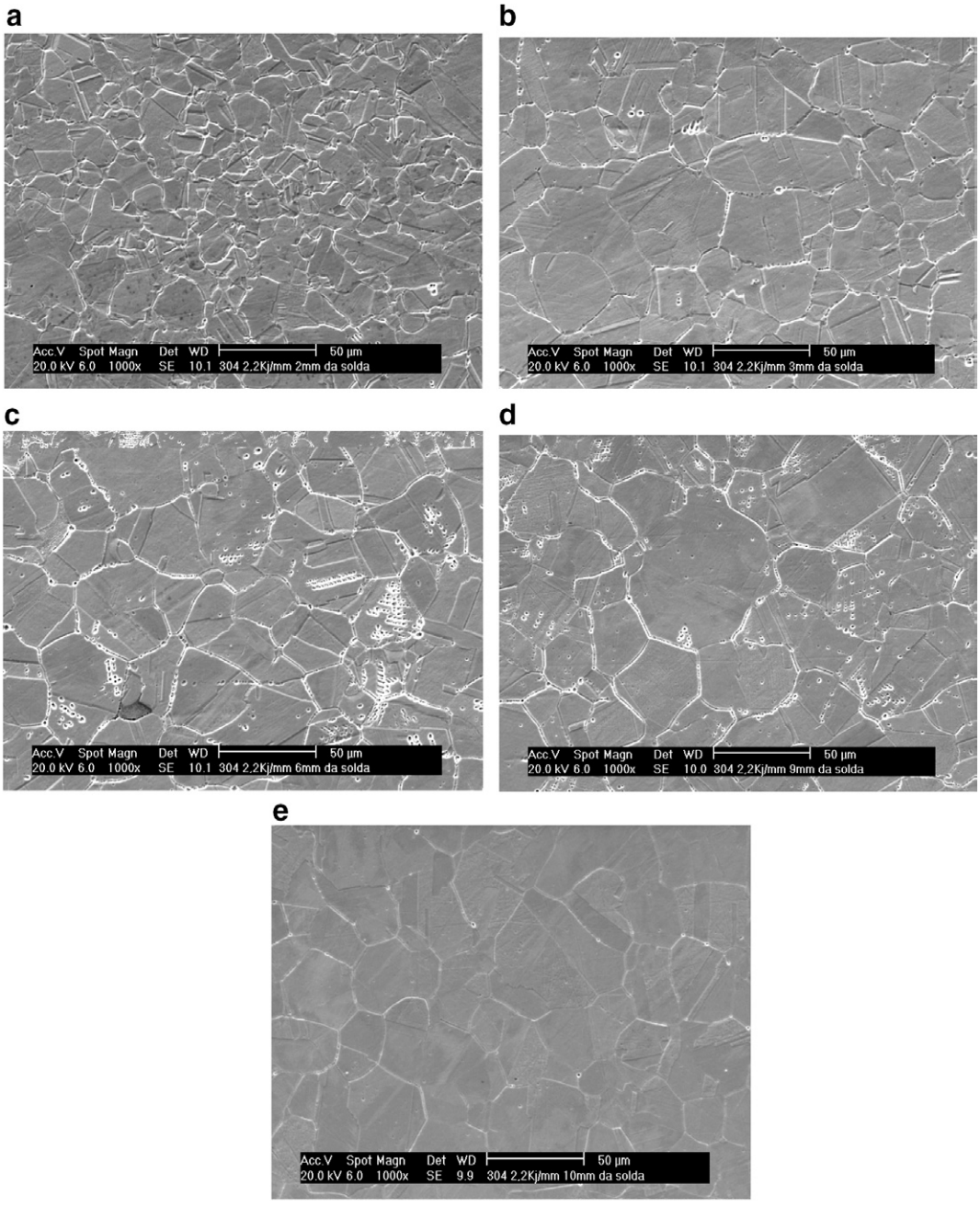

Fig. 4. SEM images showing the microstructure at different distances from the weld sting for the 304 SS welding with 2.2 kJ mm^{-1}: (a) 2 mm; (b) 3 mm; (c) 6 mm; (d) 9 mm and (e) 10 mm.

the weld string (Fig. 4a) is similar to that observed for the 304 SS welding with 0.7 kJ mm^{-2} and it is classified as step. This is an indicative that from the weld string to this distance, the temperature is higher than 800 °C. From the literature, it is known that temperatures higher than 800 °C promote the solubilisation of the chromium carbides in the grain matrix, avoiding the sensitization [1]. On the other hand, the microstructure at 3 mm from the weld string (Fig. 4b) presents some ditches around the grains characterizing a dual microstructure. This indicates that the beginning of the sensitized zone in the HAZ is at about 3 mm from the weld string. At 6 mm and 9 mm from the weld string (Fig. 4c and d), the grains are entirely surrounded by ditches and the microstructure classified as ditch, indicating that these regions of HAZ are sensitized. The images Fig. 4b and d suggest that the temperature of this HAZ region is between 800 °C and 400 °C, which leads to the precipitation of the chromium carbide in the grain boundaries. Finally, the SEM image obtained at 10 mm from the weld string (Fig. 4e) shows a microstructure similar to that observed at 2 mm from the weld string, indicating a non-sensitized region in HAZ, suggesting that the temperature of this HAZ region is lower than 400 °C HAZ and that the end of sensitized zone is around 9 mm from the weld string. The sensitized zone has an extension of 6 mm.

3.2. DLEPR test

Typical DLEPR curves obtained in the non-sensitized and sensitized regions are shown in Fig. 5. As can be observed, the difference between plots is that the curves obtained in the sensitized region shows a well defined reactivation peak in the reverse scan (Fig. 5b). The peak that appears in the reverse scan is related to the preferential breakdown of the passive film covering the chromium-depleted region of the steel. In this test, the degree of sensitization is measured by determining the ratio I_r/I_a, where I_r is the maximum current of the reverse scan and I_a is the maximum current in the forward (anodic) scan [1].

The variation of the grade of sensitization (I_r/I_a) with the distance from the weld string for the two welding energies is shown in Fig. 6. The curve shows that the steel welded with the welding energy of 0.7 kJ mm^{-1} presents the lower I_r/I_a values which remain approximately constant at about 0.004, independently of the distance. On the other hand, the value of I_r/I_a for the steel welded with 2.2 kJ mm^{-1} initially is about 0.005 until 30 mm from the weld string, followed by an increase of the I_r/I_a values with the distance reaching a maximum value of about 0.4 at 7 mm, and finally, decreases

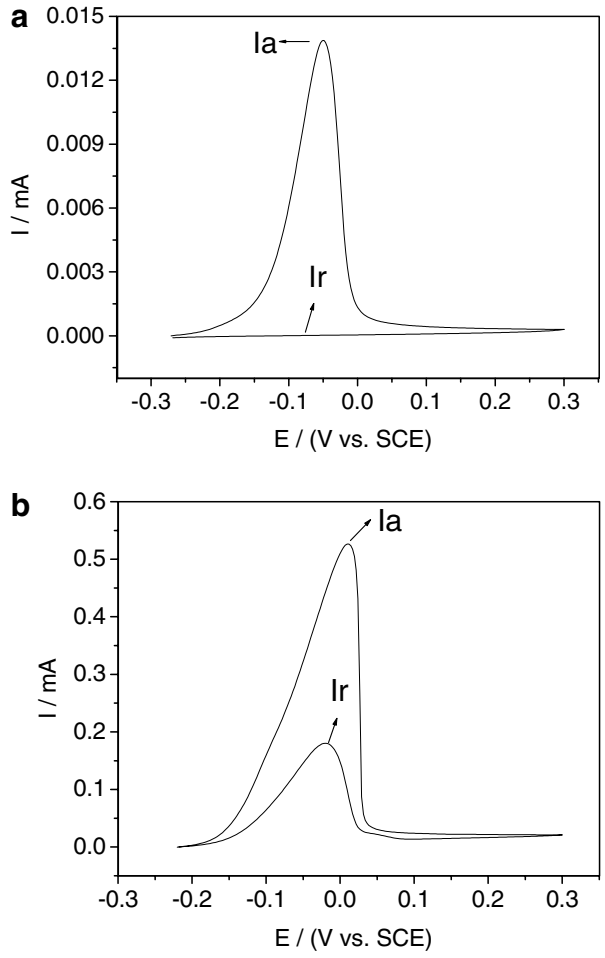

Fig. 5. DLEPR curves obtained in the non-sensitized region at 2 mm from the weld string (a) and in the sensitized region at 6 mm from the weld string (b) of the 304 stainless steel welding with 2.2 kJ mm^{-1}.

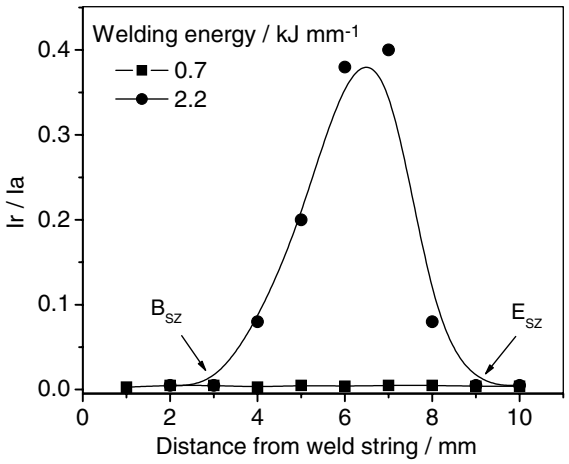

Fig. 6. Dependence of Ir/Ia with the distance from the fusion line for the two welding energies. The beginning (B_{sz}) and the end (E_{sz}) of the sensitized region are indicated.

for higher distance values until to reach the minimum value of 0.005 at 9 mm from weld string. From Fig. 6 it was confirmed that: (a) the welding energy of 0.7 kJ mm^{-1} was not enough to promote the chromium carbide precipitation in the HAZ; (b) the steel welded with the energy of 2.2 kJ mm^{-1} presents precipitation of chromium carbide in the HAZ. These results are in close agreement with those previously published by Majidi et al. [8]. Thus, the beginning (B_{sz}) and the end (E_{sz}) of the sensitized zone can be determined and are indicated in Fig. 6. The extension of the sensitized region in the steel welded with 2.2 kJ mm^{-1} is about 6 mm, which is in good agreement with the SEM analysis.

3.3. LEIS test

Fig. 7 shows examples of some local impedance diagrams obtained for the AISI 304 SS welded with both welding energy. The three diagrams in each plot were obtained at different positions from the weld string. For both systems, the diagrams are characterized in the high frequency (HF) range by a capacitive arc (not clearly defined) followed by an inductive loop, and in the lower frequency range (LF) by another capacitive part. The origin of the first capacitive loop is not yet explained. The presence of an inductive loop on the local impedance diagram was recently explained by the influence of current and potential distributions associated with the geometry of the electrode [9–11]. In addition, in a recent work, inductive loops in the HF part of the local impedance diagrams were also observed for the coupling of pure aluminium with pure copper when the probe analyzes the copper behaviour [12]. In this case, the presence of the inductive loop was connected to the existence of a galvanic coupling between the two materials, with the Cu playing the role of cathode. The coupling between Cu and Al would lead to particular current and potential distributions associated with this configuration (electric effect). By analogy with this work, it is probable that in the present study a galvanic coupling phenomenon between the weld string and the stain-

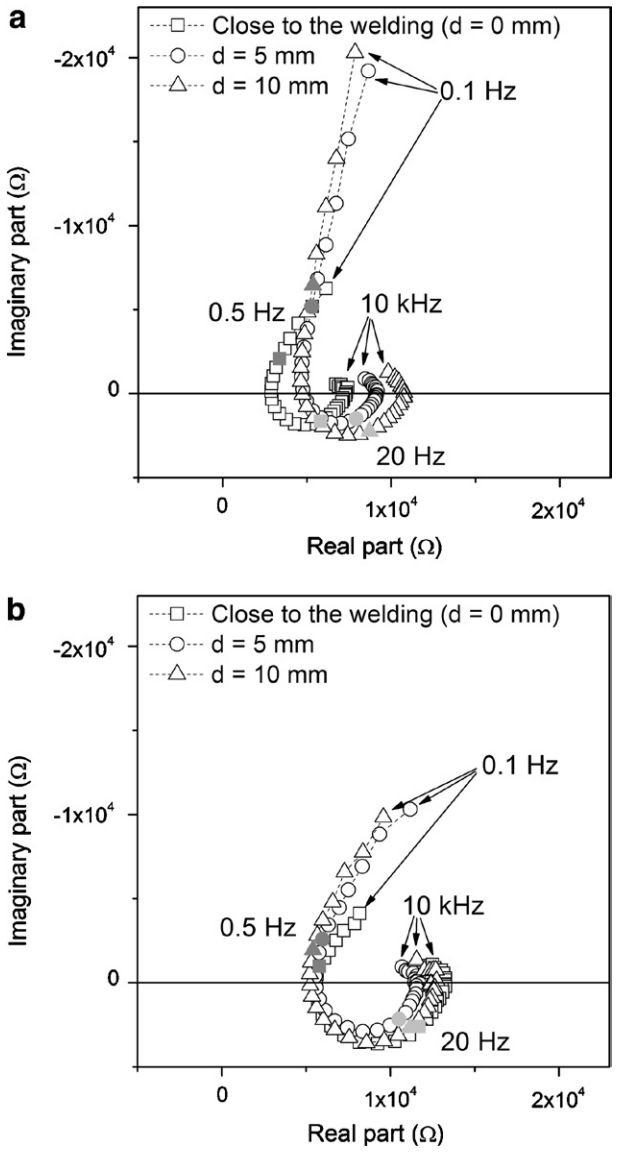

Fig. 7. Local impedance diagrams obtained on the welded 304 SS surface at different distances from the weld string: (a) welding with 0.7 kJ mm^{-1} and (b) welding with 2.2 kJ mm^{-1}.

less steel is also occurring. This assumption was reinforced by the visual observation of the plates after the electrochemical tests. Corrosion products were clearly visible close to the weld string, suggesting that the stainless steel plate could be acting as cathode in the corrosion process.

Independently of the welding energy, the diagrams plotted close to the welding (d = 0 mm) are relatively similar. This is explained by the fact that this zone is affected in the same way by the welding process. In Fig. 7a, it can be seen a purely capacitive behaviour (low frequency part of the impedance diagrams) when the probe moves away from the weld string and additionally, the diagrams are relatively similar for the two positions of the probe. On the contrary, for the AISI 304 SS welded with 2.2 kJ mm^{-1}, a frequencies shift is observed on the LF capacitive part of the diagrams when the position of the probe is changed (Fig. 7b).

To compare more easily the results obtained for the two samples, the frequency of 0.5 Hz, corresponding to the capacitive part in LF range, was chosen. Fig. 8 presents the variation of the modulus of the normalized impedance at 0.5 Hz along a line perpendicular to the weld string for the two welding energies. Measurements carried out on the welded plate with 0.7 kJ mm^{-1} constituted the reference. The impedance modulus for the reference increases gradually on the first two millimetres starting from the weld string, then its value remains relatively constant. For the welding energy of 2.2 kJ mm^{-1}, the variation of the impedance modulus can be clearly connected to the localization of the sensitized region, since it is observed a reduction in the impedance modulus for the sensitized region, compared with the SEM image (in greyed on the figure). It is observed in Fig. 3c that the welding microstructure of the stainless steel is the most sensitized at 6 mm. This point corresponds to the lowest value of the impedance modulus on Fig. 8. At 10 mm from the weld string, the microstructure is typical for a non-sensitized material (Fig. 3e). This point corresponds in Fig. 8 to a higher value of the modulus. The increase in the modulus in the vicinity of the weld string is in agreement with the microstructure observed on the Fig. 3a, which showed that in this HAZ region, the chromium carbide precipitates were dissolved in the grain matrix. For the welding energy of 2.2 kJ mm^{-1}, the values of the modulus are lower than those obtained for the welding energy of 0.7 kJ mm^{-1}. This result can be explained by some differences in the properties of the oxides formed on the stainless steel surface. The same conclusions from Fig. 8 can be made by following the variation of the impedance phase along the line perpendicular to the welding, shown in Fig 9. In the HAZ, phase values are strongly differentiated compared to those obtained for the system which is not sensitized.

Thus, the analysis of the local impedance diagram shows that the sensitized zone in the HAZ was detected by the LEIS technique at a frequency of 0.5 Hz. To visualize the

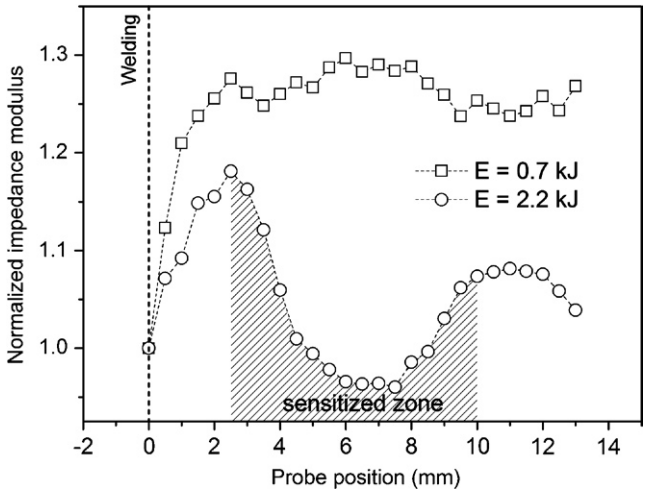

Fig. 8. Comparison of the normalized impedance modulus measured at 0.5 Hz with the distance from the weld string.

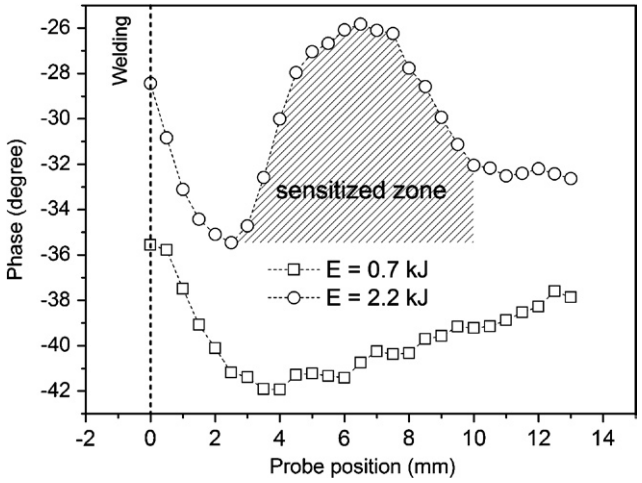

Fig. 9. Comparison of the impedance phase measured at 0.5 Hz with the distance from the weld string.

HAZ, it is necessary to work in a well defined frequency range (about the Hertz), which corresponds to interfacial phenomena.

4. Conclusions

The non-destructive DLEPR and LEIS tests allowed the length of the SZ to be determined and a very good correlation between the two techniques and the ASTM 262 Standard Practice was observed. The presence of an inductive loop on the local impedance diagrams probably reflect a galvanic coupling between the weld string (anode) and plates of the welded stainless steel (cathode) which will be very detrimental for a good corrosion resistance of the welded system. In the future, it will be necessary to obtain more information from local impedance spectra particularly regarding the high frequency part of the diagrams. The results obtained show the feasibility of developing the DLEPR and LEIS tests in industrial field.

Acknowledgments

The authors thank CNPq, ANP, FINEP and FUNCAP, Brazil, for financial assistance. Walney S. Araújo also thanks CNPq/CNRS project 490105/2004-1.

References

[1] A. John Sedriks, Corrosion of Stainless Steels, second ed., J. Wiley & Sons, 1996.
[2] S.S.M. Tavares, P. de Lima-Neto, M.P.C. Fonseca, A. Maia, J. Mater. Sci. 38 (2003) 3527.
[3] A.S. Lima, A.M. Nascimento, H.F.G. Abreu, P. de Lima-Neto, J. Mater. Sci. 40 (2005) 139.
[4] S.S.M. Tavares, V.F. Terra, P. de Lima-Neto, D.E. Matos, J. Mater. Sci 40 (2005) 4025.
[5] J.A. Souza, H.F.G. Abreu, A.M. Nascimento, J.A.C. de Paiva, P. de Lima-Neto, S.S.M. Tavares, J. Mater. Eng. Perform. 14 (2005) 367.
[6] G. Baril, C. Blanc, M. Keddam, N. Pébère, J. Electrochem. Soc. 150 (2003) B488–B493.
[7] J.-B. Jorcin, E. Aragon, C. Merlatti, N. Pèbère, Corros. Sci. 48 (2006) 1779 and references cited therein.
[8] A.Z. Majidi, M.A. Streicher, Corrosion 40 (1984) 584.
[9] V.M. Huang, V. Vivier, M.E. Orazem, N. Pébère, B. Tribollet, J. Electrochem. Soc. 154 (2007) C81–C88.
[10] V.M. Huang, V. Vivier, I. Frateur, M.E. Orazem, B. Tribollet, J. Electrochem. Soc. 154 (2007) C89–C98.
[11] V.M. Huang, V. Vivier, M.E. Orazem, N. Pébère, B. Tribollet, J. Electrochem. Soc. 154 (2007) C99–C107.
[12] J.-B. Jorcin, PhD Thesis, INP Toulouse (2007).